Supporting Information

Control of Nuclearity in Heterometallic Cu^{II}–Mn^{II} Complexes Derived from Asymmetric Schiff Bases: Structures and Magnetic Properties

Prithwish Mahapatra[a], **Sanjib Giri**[b], **Michael G. B. Drew**[c], **Ashutosh Ghosh***[,a]

[a]*Department of Chemistry, University College of Science, University of Calcutta, 92, A. P.C. Road, Kolkata 700009, India, E-mail: ghosh_59@yahoo.com*

[b]*Department of Chemistry, Sri Ramkrishna Sarada Vidyamahapitha, Kamarpukur, West Bengal 712612, India.*

[c]*School of Chemistry, The University of Reading, P.O. Box 224, Whiteknights, Reading RG6 6AD, U.K.*

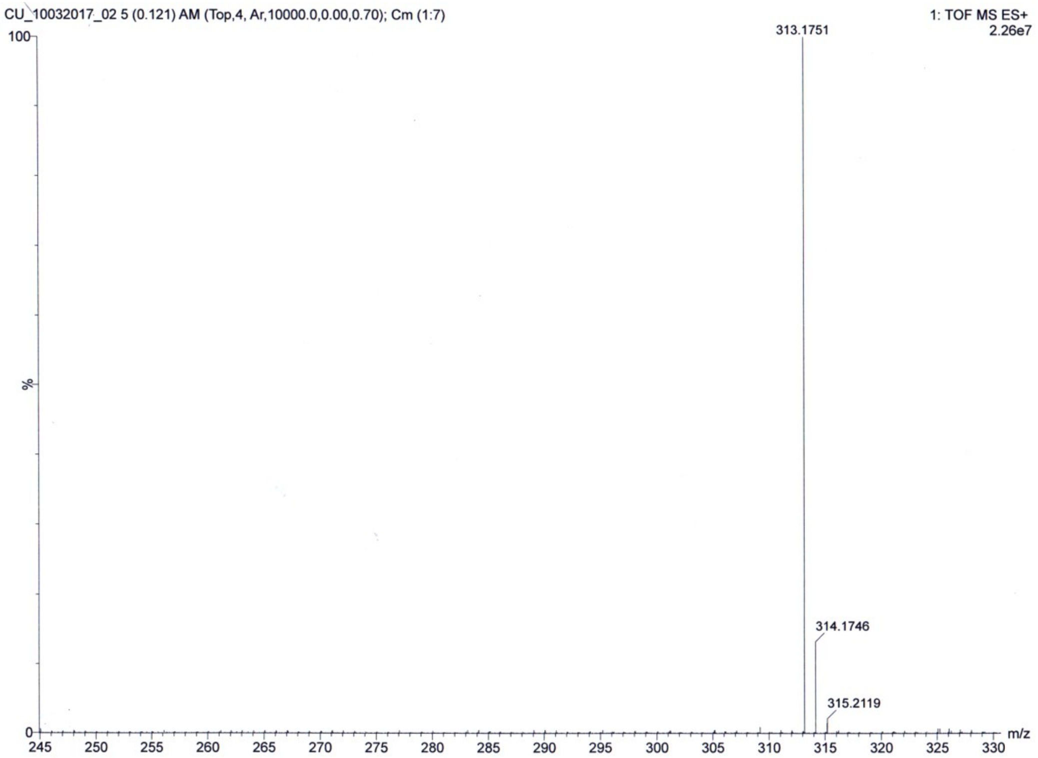

Figure S1. Representative ESI mass spectrum of ligand H_2L^2.

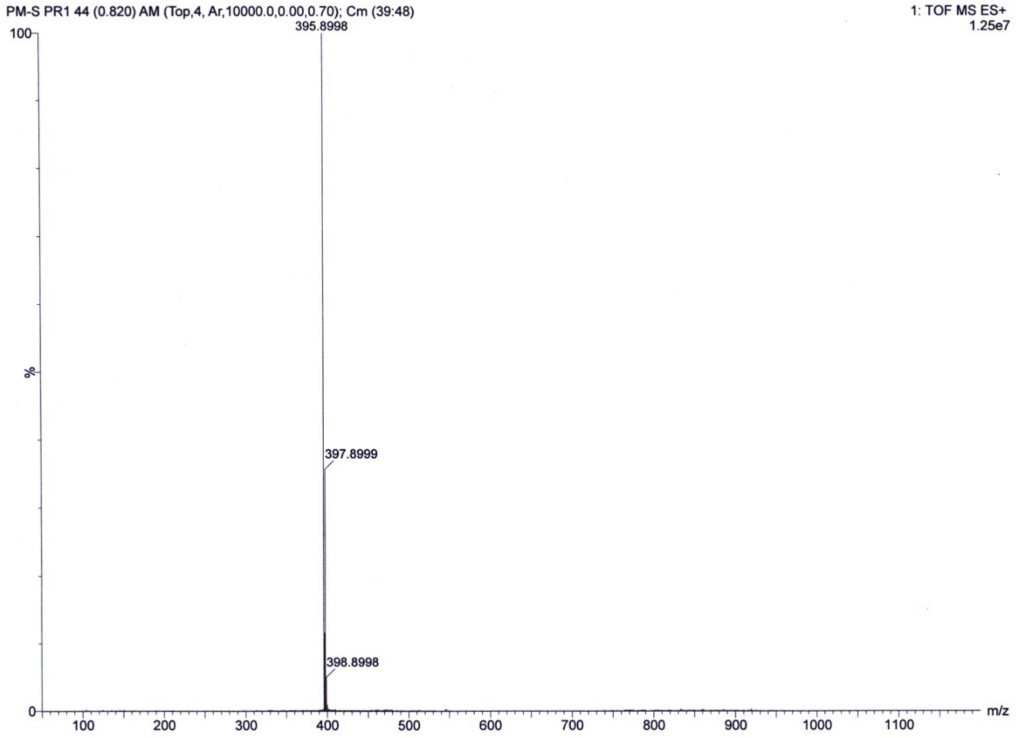

Figure S2. Representative ESI mass spectrum of ligand CuL^2.

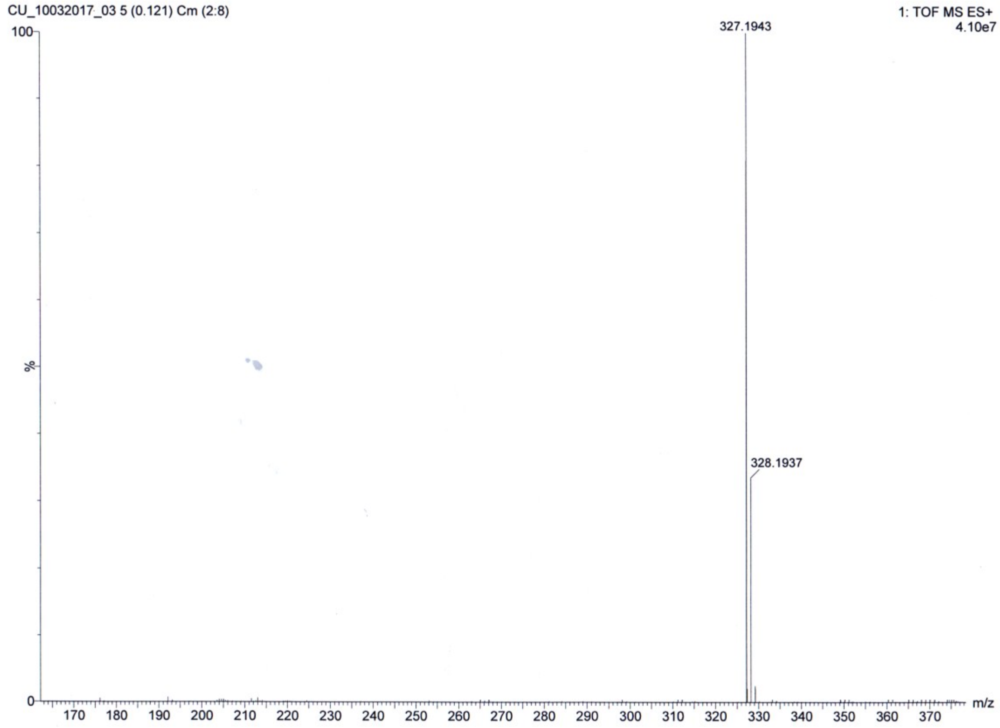

Figure S3. Representative ESI mass spectrum of ligand H_2L^3.

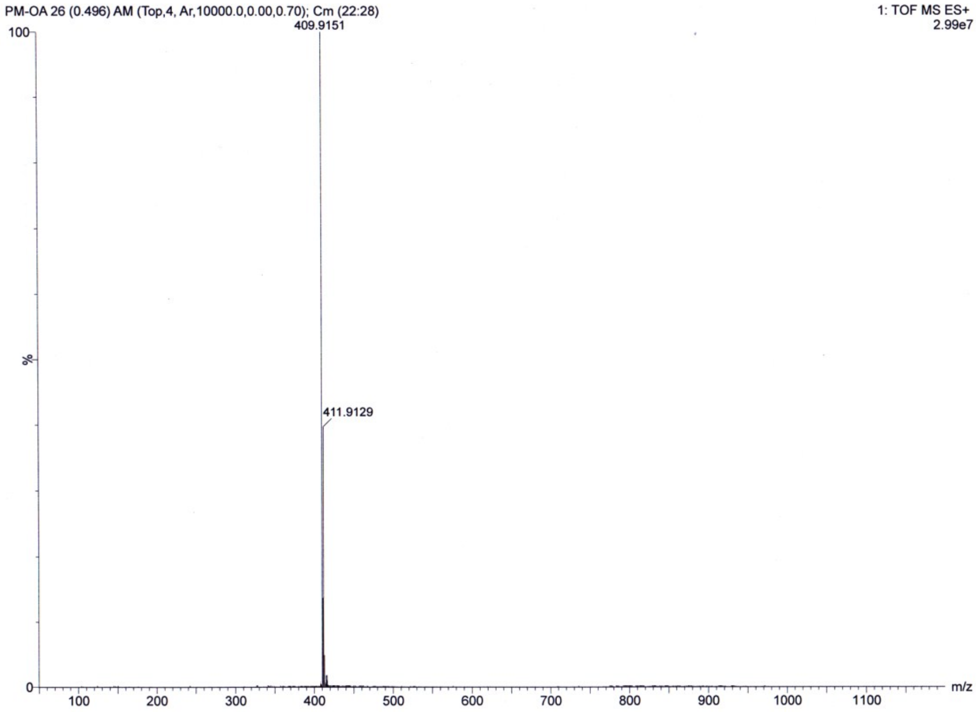

Figure S4. Representative ESI mass spectrum of ligand CuL^3.

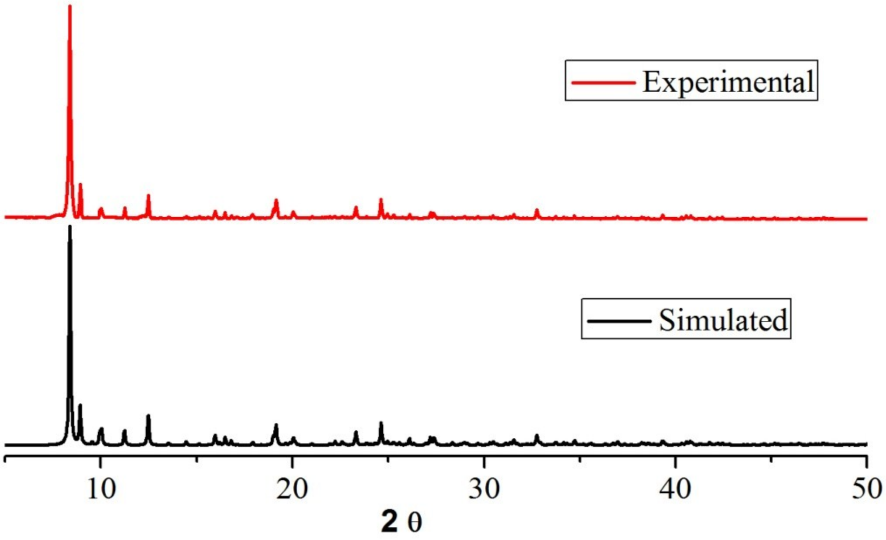

Figure S5. X-Ray powder diffractogram of complex **1**.

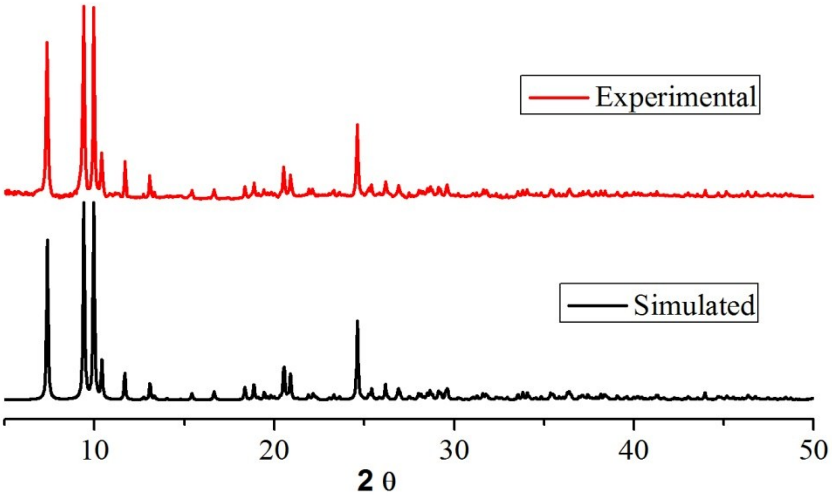

Figure S6. X-Ray powder diffractogram of complex **2**.

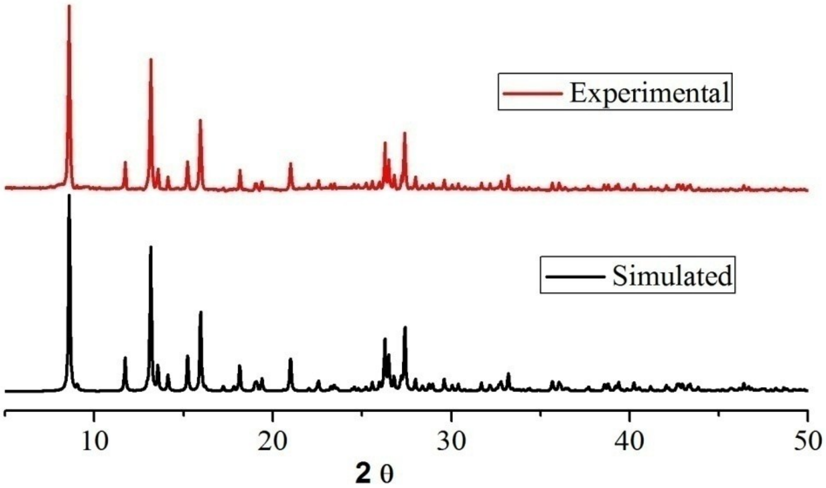

Figure S7. X-Ray powder diffractogram of complex **3**.

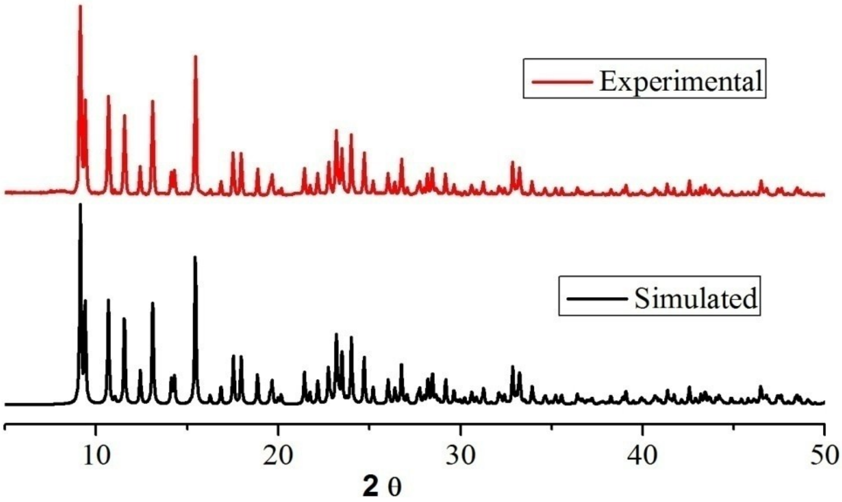

Figure S8. X-Ray powder diffractogram of complex **3**.

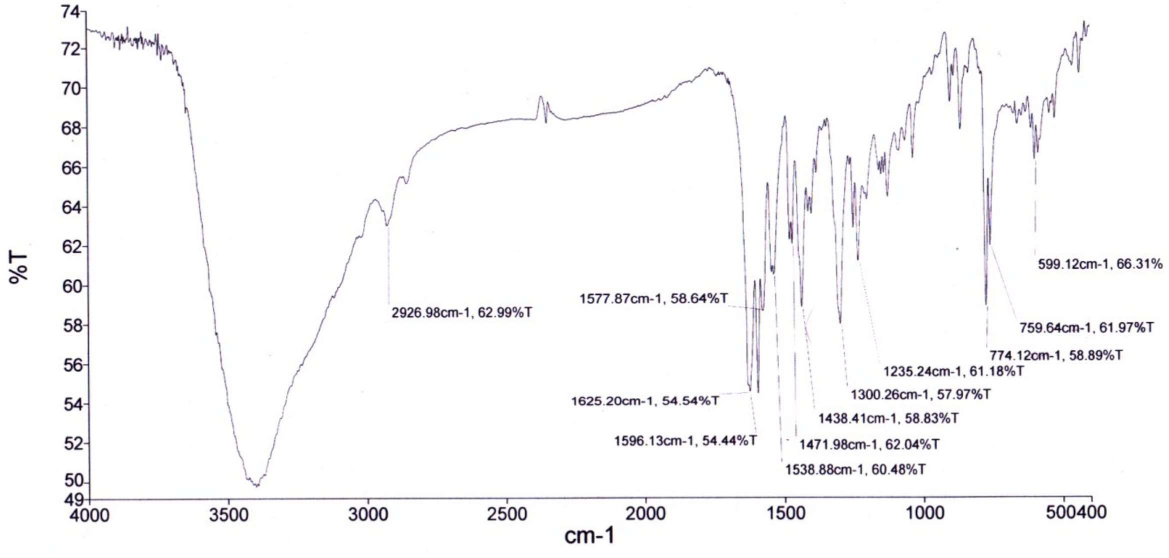

Figure S9. Representative IR spectrum of complex **1**.

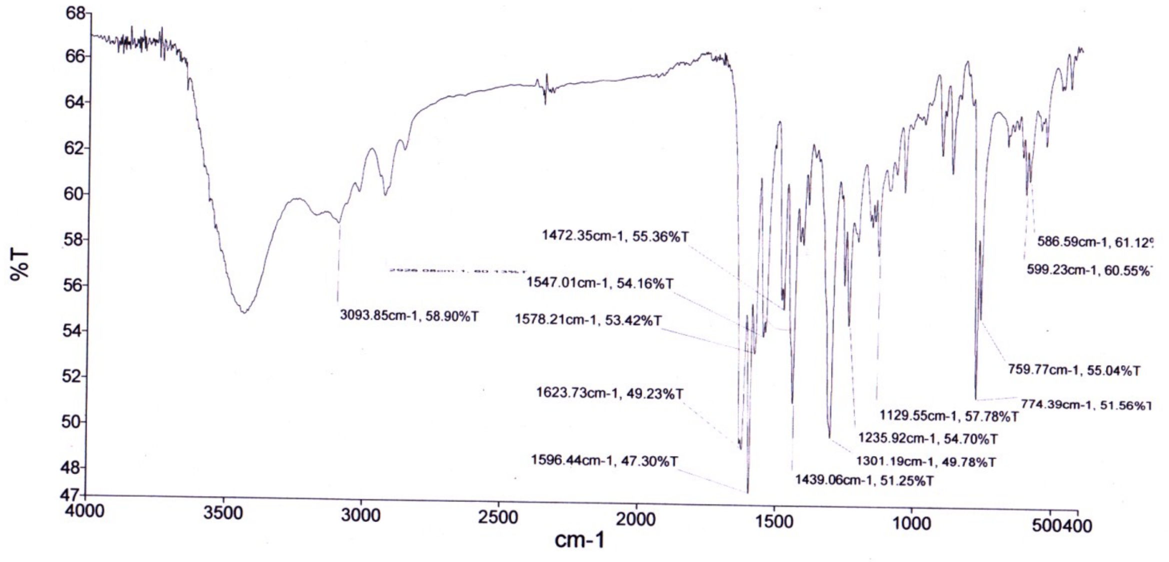

Figure S10. Representative IR spectrum of complex **2**.

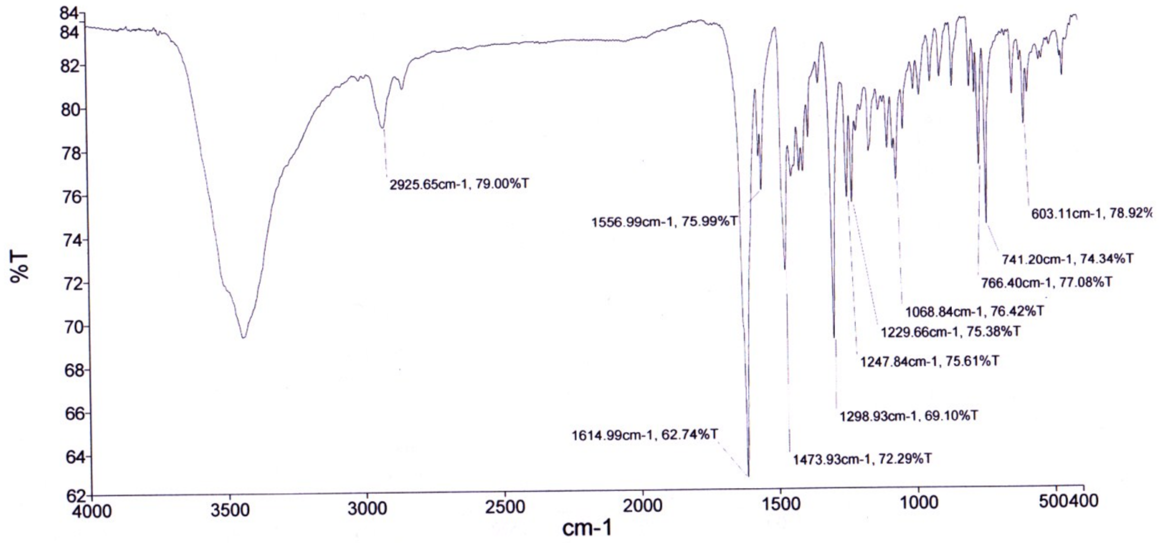

Figure S11. Representative IR spectrum of complex **3**.

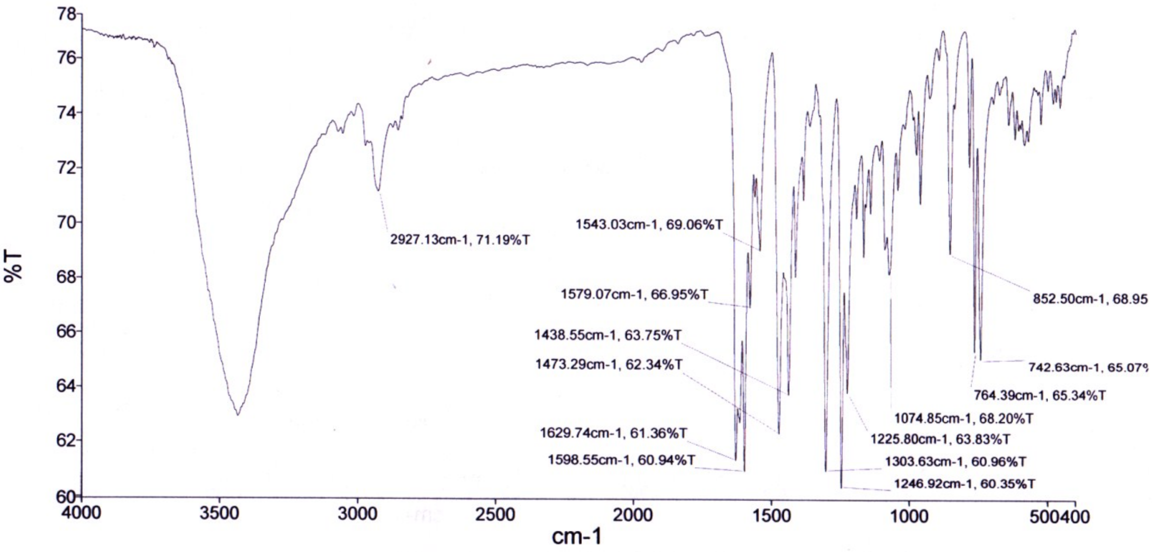

Figure S12. Representative IR spectrum of complex **4**.

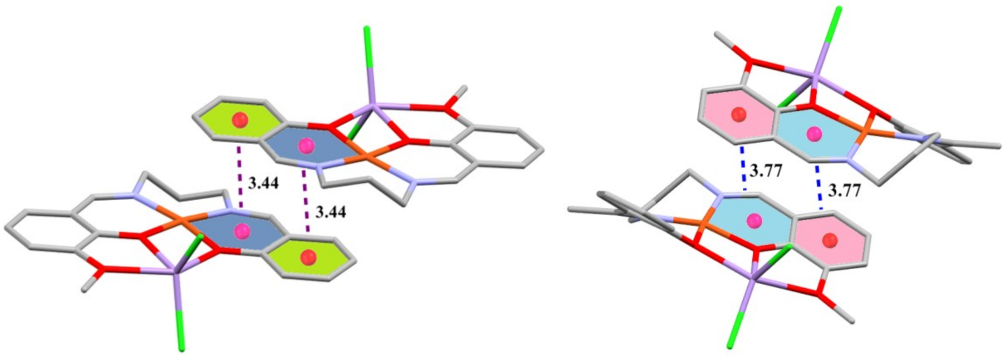

Figure S13. The weak π–π intermolecular interactions in complex **3** (left) and **4** (right).

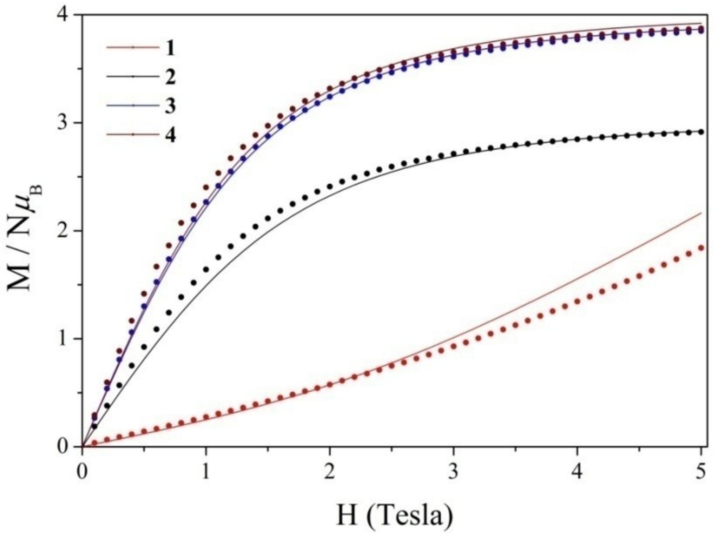

Figure S14. Isothermal magnetizations at 2 K for compounds **1–4**. Solid lines are their corresponding simulations with Brillouin function.

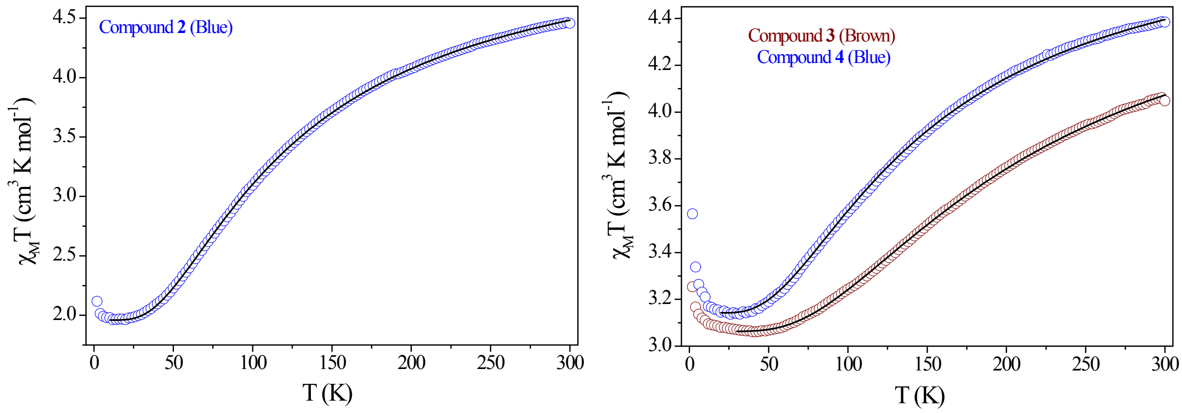

Figure S15. Variation of $\chi_M T$ as a function of temperature for complexes **2-4**. The solid lines represent the best-fit results, in 10 K-300 K range for complex **2**, in 30 K-300 K range for complex **3** and in 20 K-300 K range for complex **4** without consideration of Weiss constant parameter as described in the text.

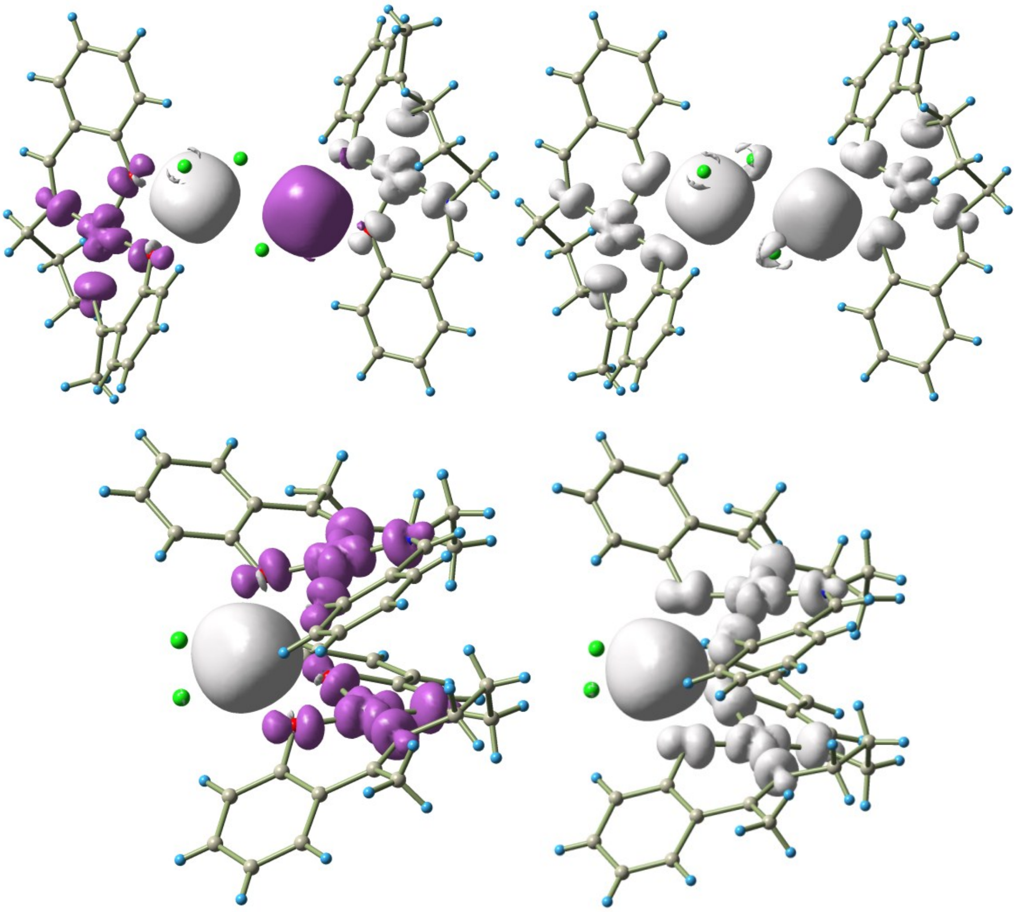

Figure S16. The calculated isodensity surfaces for lowspin (left) and highspin (right) ground state of complex **1** (upper panel) and complex **2** (lower panel) with surface cut off value 0.004 e/Å^3. Positive and negative spin densities are represented by gray and purple surfaces respectively.

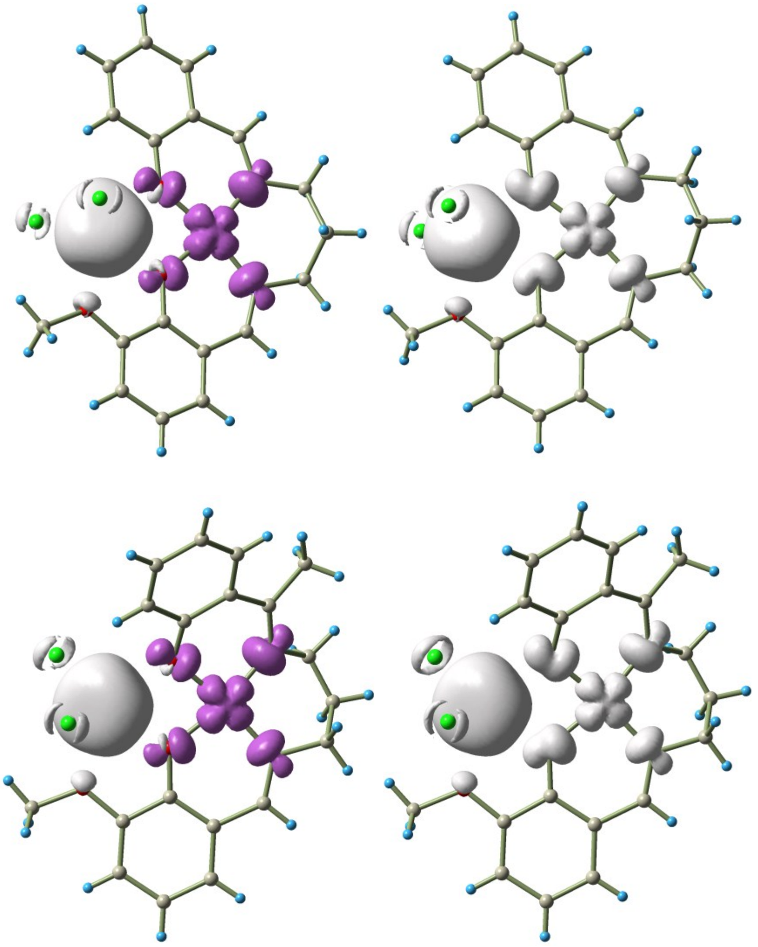

Figure S17. The calculated isodensity surfaces for lowspin (left) and highspin (right) ground of complex **3** (upper panel) and complex **4** (lower panel) with surface cut off value 0.004 e/Å^3. Positive and negative densities are represented by gray and purple surfaces respectively.

Table S1. Molecular Dimensions (Å, deg.) in the Coordination Spheres of the metals in **1**–**4**.

Compound	1	2	3	4
Cu(1)-O(1)	1.921(3)	1.922(3)	1.926(4)	1.902(4)
Cu(1)-O(2)	1.933(3)	1.936(3)	1.913(5)	1.902(3)
Cu(1)-N(1)	1.993(4)	1.996(3)	1.949(6)	1.926(5)
Cu(1)-N(2)	1.925(4)	1.955(4)	1.954(7)	1.917(5)
O(1)-Cu(1)-N(2)	172.0(2)	169.7(2)	168.4(3)	168.1(2)
O(1)-Cu(1)-O(2)	80.9(1)	82.2(1)	77.8(2)	80.7(2)

N(2)-Cu(1)-O(2)	92.7(2)	91.8(1)	90.8(3)	93.5(2)
O(1)-Cu(1)-N(1)	89.5(2)	90.4(1)	93.0(3)	93.1(2)
N(2)-Cu(1)-N(1)	97.9(2)	97.3(2)	98.4(3)	95.4(2)
O(2)-Cu(1)-N(1)	163.0(1)	165.4(1)	170.6(3)	161.6(2)
Mn(1)-O(1)	2.125(3)	2.166(3)	2.137(5)	2.199(3)
Mn(1)-O(2)	2.198(3)	2.420(3)	2.096(4)	2.116(4)
Mn(1)-Cl(1)	2.351(2)	2.454(2)	2.335(2)	2.330(2)
Mn(1)-Cl(2)	2.451(2)		2.330(2)	2.323(2)
Mn(1)-Cl(2)$1	2.520(2)			
Mn(1)-O(3)			2.282(5)	2.417(4)
O(1)-Mn(1)-O(2)	70.6(2)	66.9(1)	69.4(2)	69.6(1)
O(1)-Mn(1)-Cl(1)	112.1(1)	102.0(1)	102.7(1)	102.2(1)
O(2)-Mn(1)-Cl(1)	100.0(1)	165.7(1)	120.8(1)	126.2(1)
O(1)-Mn(1)-Cl(2)	128.6(1)		105.2(1)	110.7(1)
O(2)-Mn(1)-Cl(2)	91.0(1)		120.2(1)	117.5(1)
Cl(1)-Mn(1)-Cl(2)	118.3(1)		118.5(1)	115.0(1)
O(1)-Mn(1)-Cl(2)$1	91.4(1)			
O(2)-Mn(1)-Cl(2)$1	153.1(1)			
Cl(1)-Mn(1)-Cl(2)$1	105.4(1)			
Cl(2)-Mn(1)-Cl(2)$1	84.8(1)			
O(1)-Mn(1)-O(1)$2		137.6(2)		
O(2)-Mn(1)-O(1)$2		79.6(1)		
O(2)-Mn(1)-O(2)$2		75.1(2)		
Cl(1)-Mn(1)-O(1)$2		105.8(2)		
Cl(1)-Mn(1)-O(2)$2		94.6(1)		
Cl(1)-Mn(1)-Cl(1)$2		97.1(1)		
O(1)-Mn(1)-O(3)			140.6(2)	137.4(2)
O(2)-Mn(1)-O(3)			71.7(2)	67.9(2)
Cl(1)-Mn(1)-O(3)			97.4(2)	100.1(1)
Cl(2)-Mn(1)-O(3)			94.1(2)	91.7(1)
Symmetry elements				

$1=1-x, -y, 1-z

$2 = 1-x. y, 3/2-z

Table S2. List of fitted parameters in complexes **2**−**4** without consideration of Weiss constant.

Compounds	g_{av}	J	θ /K	R
2	2.04 (±0.05)	−39.37 (±0.07)	0	5.9×10^{-6}
3	2.02 (±0.04)	−72.73 (±0.17)	0	2.0×10^{-6}
4	2.05 (±0.05)	−49.27 (±0.14)	0	3.4×10^{-6}

Table S3. Correlations of magnetic coupling with bridging angle for earlier reported diphenoxido-bridged Mn^{II}–Cu^{II} or Cu^{II}–Mn^{II}–Cu^{II} complexes.

Complexes	Cu−O−Mn angle	J (cm^{-1})‡	CSD Code
$2(C_{20}H_{22}Cu_1N_2O_4),C_{20}H_{28}Cu_1Mn_1N_2O_7^{2+}, 2(C_{11}O_4^{1-})$	103.75	−28.0	DEXQUT
$C_{19}H_{20}Cu_1Mn_1N_4O_{10}$	107.44, 107.51	−71.6	GAJXUM
$C_{23}H_{26}Cu_1Mn_1N_2O_8$, H_2O	106.67, 107.78	−56.6	JAFLIM
$C_{26}H_{16}Cu_1F_{12}Mn_1N_2O_6$	99.57, 100.84	−22.4	LEGJAI
$C_{30}H_{43}Cu_1Mn_1N_5O_4^{2+}$, $2(C_{11}O_4^{1-})$	101.13, 101.67	−36.8	QEKFIW
$C_{22}H_{30}Cu_1Mn_1N_2O_7^{2+}$, $2(C_{22}H_{24}Cu_1N_2O_4)$, $2(C_{11}O_4^{1-})$, H_2O	103.37, 104.13	−30.4	YUVRAJ
$C_{36}H_{30}Cu_2Mn_1N_4O_8,5(H_2O)$	103.28, 101.68	−28.5	BIXXEM
$C_{38}H_{40}Cu_2Mn_1N_{10}O_4$	91.84, 103.54	−20.0	FANJAH
$C_{40}H_{40}Cu_2Mn_1N_6O_6$	91.27, 103.25	−17.3	FANJEL
$C_{40}H_{40}Cu_2Mn_1N_6O_4S_2$	92.47, 103.35	−32.5	FANJIP
$C_{36}H_{32}N_6O_6Cu_2Mn_1$	98.62, 103.27	−26.5	QILDOG
$C_{36}H_{36}Cu_2Mn_1N_7O_5,ClO_4,O$	96.2, 102.9	−43.6	HAWPED
$C_{38}H_{36}Cu_2Mn_1N_6O_4S_2$	97.27, 103.80	−44.6	HAWPIH

Table S4. Mulliken spin densities (in au) for high-spin (HS) and broken symmetry spin (BS) states of complexes **1**–**2**.

Complex **1**			Complex **2**		
Selected atoms	HS	BS	Selected atoms	HS	BS
Cu1	0.59015	−0.56211	Cu1	0.59097	−0.56612
Mn1	4.81687	4.79916	Mn1	4.8303	4.80991
Mn1′	4.81684	−4.79913	Cu2	0.59098	−0.56613
Cu1′	0.59014	0.56211	Cl1$_{(coordinating)}$	0.05792	0.05398
Cl1$_{(coordinating)}$	0.07013	0.0698	Cl2$_{(coordinating)}$	0.05791	0.05397
Cl2$_{(bridging)}$	0.06527	0.00547	O1$_{(bridging)}$	0.10428	−0.10343
Cl1′$_{(bridging)}$	0.07014	−0.06981	O2$_{(bridging)}$	0.09932	−0.10246
Cl2′$_{(coordinating)}$	0.06527	−0.00547	N1$_{(coordinating)}$	0.09471	−0.09012
O1$_{(bridging)}$	0.09863	−0.08519	N2$_{(coordinating)}$	0.10522	−0.09956
O2$_{(bridging)}$	0.10133	−0.09846	O3$_{(bridging)}$	0.10427	−0.10341
N1$_{(coordinating)}$	0.10644	−0.10035	O4$_{(bridging)}$	0.09932	−0.10247
N2$_{(coordinating)}$	0.10775	−0.10066	N3$_{(coordinating)}$	0.09474	−0.09014
O1′$_{(bridging)}$	0.09862	0.08519	N4$_{(coordinating)}$	0.10522	−0.09955
O2′$_{(bridging)}$	0.10132	0.09843			
N1′$_{(coordinating)}$	0.10644	0.10035			
N2′$_{(coordinating)}$	0.10777	0.10067			

Table S5. Mulliken spin densities (in au) for high-spin (HS) and broken symmetry spin (BS) states of structures **3**–**4**.

	Complex **3**		Complex **4**	
Selected atoms	HS	BS	HS	BS
Mn1	4.79938	4.78044	4.80816	4.79874
Cu1	0.60645	–0.5706	0.59161	–0.567
O1 $_{(\mu\text{-}1,1\text{-}phenoxido)}$	0.099	–0.09315	0.10815	–0.10307
O2 $_{(\mu\text{-}1,1\text{-}phenoxido)}$	0.09013	–0.07619	0.08651	–0.07845
O3 $_{(\mu\text{-}1,1\text{-}methoxido)}$	$–3.7\times10^{-5}$	$–7.27\times10^{-4}$	$–1.89\times10^{-4}$	–0.00108
N1$_{(coordinating)}$	0.11124	–0.10186	0.12072	–0.11565
N2$_{(coordinating)}$	0.11494	–0.10099	0.10465	–0.09425

Cl1(*coordinating*)	0.06612	0.06605	0.06684	0.06636
Cl2(*coordinating*)	0.06725	0.06747	0.06824	0.06815
C17(*adjacent to-methoxido*)	0.01492	-4.66×10^{-4}	0.01375	-7.64×10^{-4}
C18 (*adjacent to-phenoxido O2*)	–0.00234	3.4×10^{-5}	6.1×10^{-4}	0.0029